Available online at www.sciencedirect.com

ScienceDirect

Procedia Materials Science 3 (2014) 1579 – 1584

Procedia Materials Science

www.elsevier.com/locate/procedia

20th European Conference on Fracture (ECF20)

Nonlinear Damage Identification in Fiber-Reinforced Cracked Composite Beams through Time-Space Wavelet Analysis

Andrea Spagnoli[a]*, Lorenzo Montanari[a], Biswajit Basu[b], Brian Broderick[b]

[a]*Department of Civil-Environmental Engineering and Architecture, Parco Area delle Scienze 181/A, 43124 Parma, Italy*
[b]*Department of Department of Civil, Structural and Environmental Engineering, Trinity College, Dublin 2, Ireland*

Abstract

It is well-known that wavelet analysis is, in the space domain, an efficient way to determinate the damage location (Pakrashi et al., 2007; Loutridis et al., 2004), while, in the time domain, it is an efficient tool to identify the system stiffness variation (Hou et al., 2000; Basu et al., 2008). Based on the idea of combining the information of the structural response in both space and time domains, a new time-space wavelet-based technique aimed at identifying the nonlinear behaviour of damage for SHM is presented. A FE model of a fiber-reinforced cantilever beam with a bridged crack is used to simulate the nonlinear static structural response. On the basis of particular conditions related to the Continuous Wavelet Transform (CWT) of the beam deflection and of the features of the 4th order Coiflets wavelet, a linear relation between the values of the relative rotation due to the crack and the normalized wavelet coefficients at the crack position is ruled out. By analysing through CWT the time sequence of the beam response in the space domain through the aforementioned linear relation, the nonlinear structural behaviour due to damage is identified. The effectiveness of the method in calibrating a small crack, is discussed with respect to the wavelet scale and the noise level.

Keywords: fiber-reinforced composite, bridged-crack model, wavelet analysis, space-time domains, nonlinear damage identification.

* Corresponding author. Tel.: +39-0521-905927; fax: +39-0521-905924.
E-mail address: spagnoli@unipr.it

Selection and peer-review under responsibility of the Norwegian University of Science and Technology (NTNU), Department of Structural Engineering
doi:10.1016/j.mspro.2014.06.255

1. Damaged Beam Modelling

A FE model is used to simulate the static deflection, due to a concentrated end force $P(t)$, of a fiber-reinforced cantilever beam with a rectangular cross-section and a bridged edge crack (Fig. 1a). The composite matrix presents a linear-elastic behaviour, while a fracture mechanics-based theoretical model (Carpinteri An. et al., 2004; Spagnoli et al., 2014) is used to describe the elastic-plastic response of the cracked beam section due to the applied bending moment and crack bridging reactions due to fibers.

Two-node Timoshenko beam finite elements with coupled transversal displacements and rotations (Friedman & Kosmatka, 1993) are employed in the FE model. The uncracked elements have linear-elastic bending and shear behaviour; while the cracked element (Viola et al., 2002), represented by a rotational spring of stiffness $k_c(t)$ at its mid-length, behaves in a nonlinear manner.

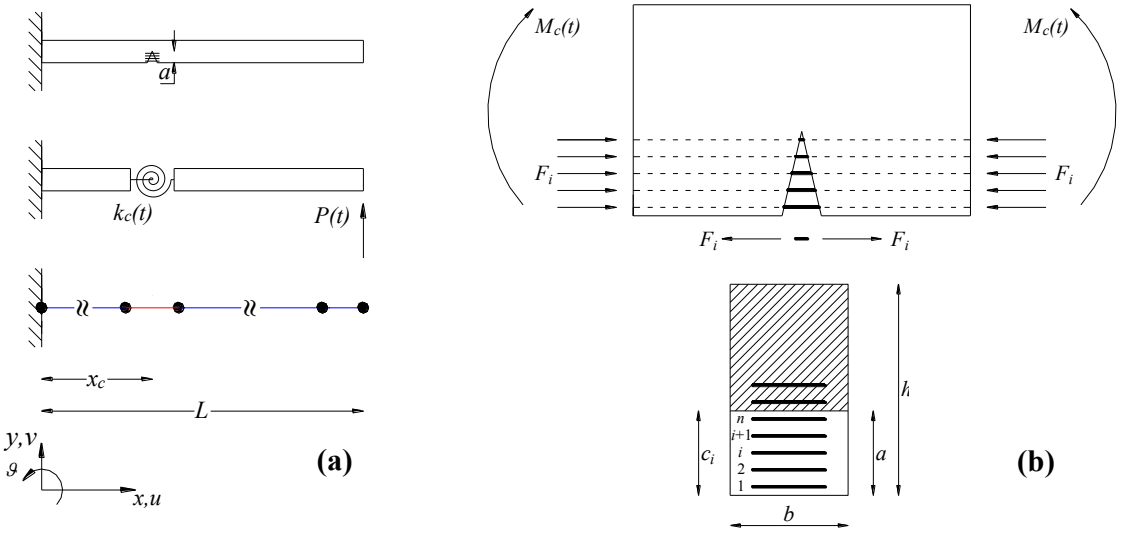

Fig. 1. (a) Sketch of the FE model of a generic fiber-reinforced cantilever beam with a bridged crack; (b) schematic of the bridged crack model.

In fibrous composite materials with a brittle matrix, fibers produce a bridging action on crack faces which affects the global structural response in the cracking phase. To take into account this behaviour, the sectional bridged crack model proposed by Carpinteri et al. (2004) is used. Let us consider a through-thickness edge crack in a fiber-reinforced composite cantilever beam with a rectangular cross-section. The crack is at a distance x_c from the clamped end and is located in the tensile part of the beam. The crack is subjected to Mode I loading due to the cross-section bending moment $M_c(t)$, in equilibrium with the applied force $P(t)$, and to the fiber bridging forces (Fig. 1b).

Unidirectional fibers are discretely distributed across the crack and oriented parallel to the longitudinal axis of the beam. The position of the i-th fiber ($i = 1,\ldots,n$) is described by the distance ci with respect to the bottom of the beam cross-section. Further, the relative crack depth $\xi = a / h$ and the normalized coordinate $\zeta_i = c_i / h$ are defined. The matrix of the beam is assumed to present a linear elastic behaviour, whereas the fibers act as rigid-perfectly plastic bridging elements which connect together the two surfaces of the crack. Hence, the plastic bridging law for the generic i-th fiber is characterized by an ultimate force $F_{P,i}$ (and $-F_{P,i}$ in compression).

Since the problem is statically indeterminate, the unknown fiber reactions, F_i , (positive if the fiber is under tensile loading) on the matrix can be deduced from n kinematic conditions related to the crack opening displacements w_i at the different fiber locations (Spagnoli et al., 2014). If $|F_i|$ is equal to $F_{P,i}$, the force in the i-th fiber is known, and the crack opening displacements are hereafter shown to depend on such a value. Since the matrix is assumed to behave in a linear elastic manner, the crack opening displacement, w_i , at the i-th fiber level is

computed through the superposition principle:

$$\mathbf{u} = \boldsymbol{\lambda}_{\mathbf{M}} M_c + \boldsymbol{\lambda}\,\mathbf{F} \tag{1}$$

where $\mathbf{u} = \{u_1,\ldots,u_n\}^T$ is the vector of the crack opening displacements at the different fiber levels, and $\mathbf{F} = \{F_1,\ldots,F_n\}^T$ is the vector of the crack bridging forces. Further, $\boldsymbol{\lambda}_{\mathbf{M}} = \{\lambda_{1M},\ldots,\lambda_{nM}\}^T$ is the vector of the compliances related to the bending moment M_c, whereas $\boldsymbol{\lambda}$ is a symmetric square matrix of order n, whose generic element *ij* represents the compliance λ_{ij} related to the *i*-th crack opening displacement and the *j*-th fiber force (see Carpinteri A. et al., 2004). All the compliance coefficients turn out to be inversely proportional to the Young modulus of the matrix E_m.

The incremental form of Eq. 1 is (summation rule for repeated indices holds) (Spagnoli et al., 2014):

$$\dot{u}_i = \lambda_{iM}\,\dot{M}_c - \lambda_{ij}\,\dot{F}_j \quad \text{with} \quad i = 1,\ldots,n \tag{2}$$

where the dot symbol indicates a time derivative, with $F_i = \int \dot{F}_i\,dt$ and $u_i = \int \dot{u}_i\,dt$. If the general *i*-th fiber is in the elastic domain, the corresponding increment of crack opening displacement $\dot{u}_i$ is null, namely if $|F_i| < F_{P,i} \Rightarrow \dot{u}_i = 0$. On the other hand, if the general *i*-th fiber is yielded ($|F_i| = F_{P,i}$), the following two alternatives are possible: $\dot{F}_i = 0 \Rightarrow F_i\,\dot{u}_i > 0$ or $F_i\,\dot{F}_i < 0 \Rightarrow \dot{u}_i = 0$ (plastic-to-elastic return). In other words,

$$F_i\,\dot{u}_i > 0 \ \text{ if } |F_i| = F_{P,i} \text{ and } \dot{F}_i = 0\,; \qquad \dot{u}_i = 0 \ \text{ otherwise} \tag{3}$$

Once the incremental crack bridging forces are known, the incremental relative rotation $\Delta\dot{\vartheta}_c$ of the cracked section is given by:

$$\Delta\dot{\vartheta}_c = \lambda_{MM}\,\dot{M}_c - \lambda_{iM}\,\dot{F}_i \tag{4}$$

where λ_{MM} is the rotational compliance due to the bending moment. As $\Delta\vartheta_c = \int \Delta\dot{\vartheta}_c\,dt$ is the relative rotation of the crack section at time *t*, the lumped crack rotational stiffness $k_c(t)$ is evaluated through the relation:

$$k_c(t) = M_c(t) / \Delta\vartheta_c(t) \tag{5}$$

In order to accommodate the bridged crack model within the framework of the FE method, a two-node Timoshenko cracked beam element with 4 degrees of freedom is used (Viola et al., 2002). The element is constituted by two solid portions connected at mid-length by a rotational spring of stiffness k_c. The stiffness matrix K_c of the cracked beam element is as follows

$$K_c = \begin{bmatrix} \frac{12EI}{l_c^3(1+\Gamma)} & \frac{6EI}{l_c^2(1+\Gamma)} & -\frac{12EI}{l_c^3(1+\Gamma)} & \frac{6EI}{l_c^2(1+\Gamma)} \\ \frac{6EI}{l_c^2(1+\Gamma)} & EI\left(\frac{3}{l_c(1+\Gamma)}+\frac{1}{EI/k_c+l_c}\right) & -\frac{6EI}{l_c^2(1+\Gamma)} & EI\left(\frac{3}{l_c(1+\Gamma)}-\frac{1}{EI/k_c+l_c}\right) \\ -\frac{12EI}{l_c^3(1+\Gamma)} & -\frac{6EI}{l_c^2(1+\Gamma)} & \frac{12EI}{l_c^3(1+\Gamma)} & -\frac{6EI}{l_c^2(1+\Gamma)} \\ \frac{6EI}{l_c^2(1+\Gamma)} & EI\left(\frac{3}{l_c(1+\Gamma)}-\frac{1}{EI/k_c+l_c}\right) & -\frac{6EI}{l_c^2(1+\Gamma)} & EI\left(\frac{3}{l_c(1+\Gamma)}+\frac{1}{EI/k_c+l_c}\right) \end{bmatrix} \tag{6}$$

where *E* is the equivalent Young modulus of the composite material, *I* is the moment of inertia of the cross-section, l_c is the length of the cracked finite element and $\Gamma = 12EI\chi/GAl_c$ is the shear deformation parameter of the beam, with χ being the shear coefficient (equal to 1.2 for a rectangular cross-section), *G* the shear elastic modulus of the matrix and *A* the cross-sectional area.

2. Time-space wavelet-based nonlinear damage identification

2.1. Wavelet analysis

A wavelet function $\psi(x)$ is a zero mean local wave-like function which decays rapidly and must satisfy some

particular conditions (Mallat, 2001). These functions, thanks their multi-resolution features, are suitable to analyse the details of non-stationary signals. The Continuous Wavelet Transform (CWT) is here employed as a tool to characterize the damage behavior in beam deflections. The CWT is defined by the convolution of the beam deflection $\eta(x)$ with a wavelet function generated from the mother wavelet $\psi(x)$ by scaling and translating it (Mallat, 2001):

$$W(t,s) = \int_{-\infty}^{+\infty} v(x) \frac{1}{\sqrt{s}} \psi^* \left(\frac{x-t}{s} \right) dx \tag{7}$$

where t and s are respectively the translation and scale parameters, and ψ^* is the complex conjugate of ψ. Throughout the paper the 4th order of Coiflets wavelet ('Coif4') is adopted.

2.2. Normalized CWT coefficients and crack relative rotation

It can be demonstrated (Montanari, 2014) that when the coefficients of the wavelet transform attain negligible values in the undamaged parts of the beam in comparison with those close to the crack location (this happens when the crack discontinuity due to relative rotation alters significantly the beam curvature), the value of the normalized CWT coefficient ($\overline{W}(t,s) = W(t,s)/dx^2$, where dx is the sampling interval of the beam deflection) at the crack location depends, with good approximation, on the value of the crack relative rotation and on the analyzing wavelet scale.

The bilogarithmic graph of Fig. 2a shows that there is a linear dependence between the relative rotation due to the crack, $\Delta\vartheta_c$, and the normalized CWT coefficients at the crack location x_c, $\overline{W}(x_c,s)$ (when $\overline{W}(x \neq x_c,s) \ll \overline{W}(x_c,s)$), function of the scale s. Representing the curves of Fig. 2a, related to a certain crack rotation range, in a bilinear graph (e.g. see Fig. 2b), we obtain approximately straight lines, passing through the origin and characterized by different values of the angular coefficient, $\Theta(s)$, dependent on the wavelet function and the scale s, that is:

$$\overline{W}(x_c,s) = \Theta(s)\Delta\vartheta_c \tag{8}$$

In Fig. 2c the trend of $\Theta(s)$ against the wavelet scale is illustrated.

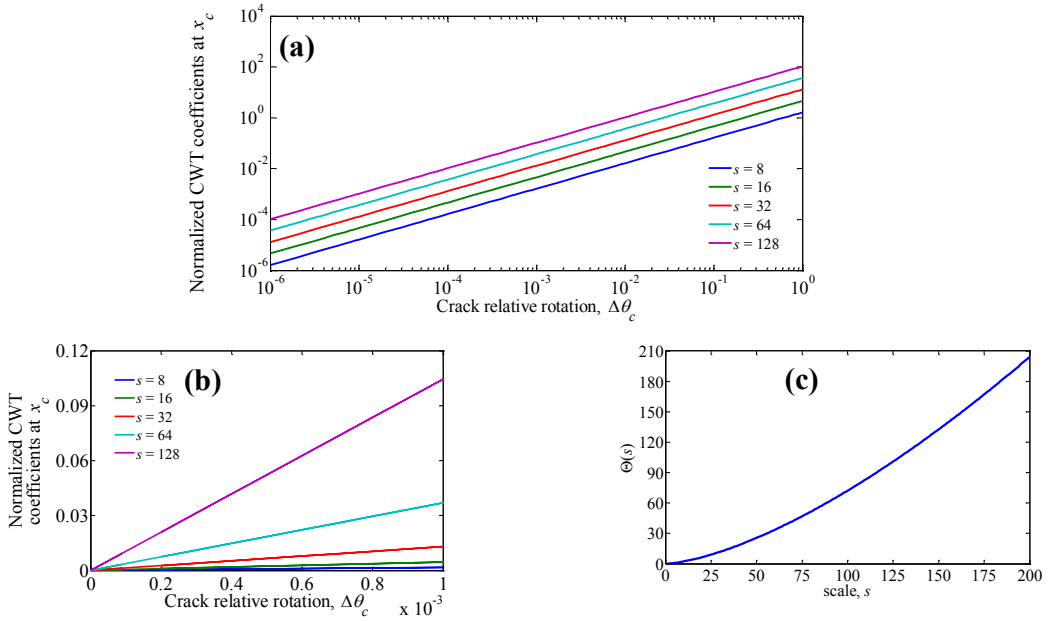

Fig. 2. Relation between the normalized CWT coefficients at the crack location x_c and the relative rotation due to the crack. Different scales s are considered. (a): bilogarithmic graph; (b) bilinear graph in the range $\Delta\vartheta_c$ = [0 – 0.001] rad; (c) Trend of the function $\Theta(s)$.

2.3 Identification method of the nonlinear crack behaviour

The time-space wavelet-based damage identification method presented in Montanari (2014) allows the description of the nonlinear crack behaviour in terms of relative rotation of the crack itself. The technique requires the availability of the beam response both in time and in space at rather dense intervals. Furthermore, the crack discontinuity has to be such that the wavelet transform can locate it by means of a peak of its coefficients markedly higher than the coefficient values along the undamaged parts of the beam. The method operates as following, at each time step:

(i) the beam deflection, opportunely padded to avoid edge effects, is analysed through CWT;
(ii) the wavelet coefficient value at the crack location (which has to be known a priori) is normalized with respect to the square of the spatial interval dx;
(iii) the crack relative rotation $\Delta\vartheta_c$ is determined through Eq. 8, knowing the value of $\Theta(s)$.

Once the time history of the crack relative rotation is extracted, the evolution of damage can be determined through an appropriate mechanical model.

3. Illustrative example

The damage calibration method is applied to numerical data which simulate the static responses of a cracked fiber-reinforced composite beam subjected to a point load $P(t)$ at the free end (see Fig. 1a). A cracked beam reinforced with long unidirectional fibers equally distributed in the matrix with a volume fraction v_f of 10% is considered. The beam has length L = 2 m, height h = 0.2 m and width b = 0.15 m. The matrix has Young's modulus E_m and Poisson coefficient v_m, respectively, equal to 30 GPa and 0.15. The fibers are characterized by diameter of 30 μm, Young's modulus E_f of 80 GPa and yield stress of 2000 MPa. The Young's modulus of the composite is equal to $E_{eq} = (1 - v_f)E_m + v_f E_f = 35$ GPa. The crack has a relative depth $\delta = a/h = 10\%$ and is located at $x_c/L = 0.1$.

The beam deflection shapes are sampled at the sampling intervals dx = 0.001 m and, to simulate real measurement data, synthetic Gaussian white noise is added (different SNR values are imposed). The deflections of the static analysis are sampled at each variation $\Delta P = \pm 2000$ N of the acting load $P(t)$.

The load history of Fig. 4a is considered and SNR = 120dB is assumed. Firstly, the wavelet scale providing the best estimation of the crack relative rotation is determined. Different scale values are investigated, i.e. s = 10, 30, 60, 90 and 120. Figure 4b displays the rotational stiffness of the crack section.

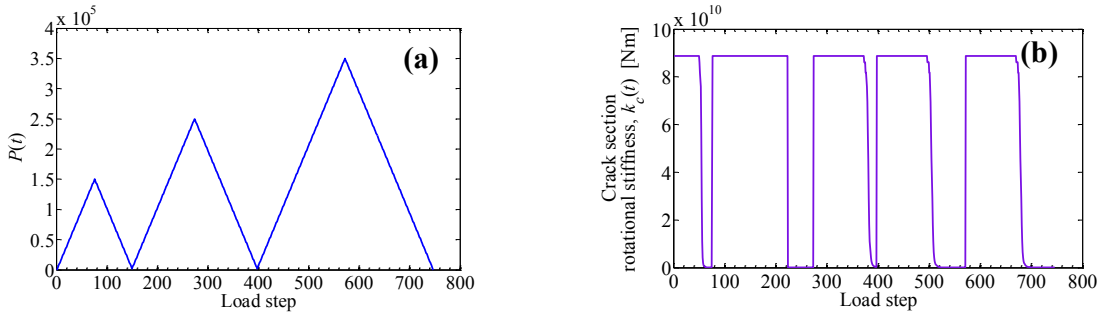

Fig. 3. (a) Load history; (b) history of the rotational stiffness of the crack section.

In Fig. 4a the history of the crack relative rotation $\Delta\vartheta_c$ estimated by the wavelet-based calibration method at different scales is illustrated. Figure 5b reports the normalized CWT coefficients at a position far from the crack location (say, x/L = 0.7) divided by $\Theta(s)$ for different wavelet scales. By juxtaposing the results of Fig. 4a with those of Fig. 4b, one can verify that the proposed calibration method is applicable. In fact, the value of the CWT coefficients at beam points far away from the crack location and the beam ends are at least one order of magnitude smaller than those at the crack section for the considered scales.

It can be demonstrated (Montanari, 2014) that scale 120 identifies higher values of $\Delta\vartheta_c$, due to the influence of the edge effects. Among the scales 10, 30, 60 and 90, scale 60 is chosen to estimate $\Delta\vartheta_c$ as it averages the

estimations of the other scales. Figure 5a highlights that the wavelet-based calibration method using $s = 60$ describes accurately the history of the crack relative rotation simulated by the FE model.

Let us now consider the same problem but with an increasing noise level (SNR equal to 100 and 80 dB is imposed). Figure 5b shows that the calibration method at SNR = 100 dB provides still a good description of the history of the crack relative rotation. At SNR = 80 dB, the history of $\Delta\vartheta_c$ is sensibly influenced by the presence of noise, but an approximate quantification of the values of $\Delta\vartheta_c$ can still be carried out (a smoothing post-processing of the data could be helpful).

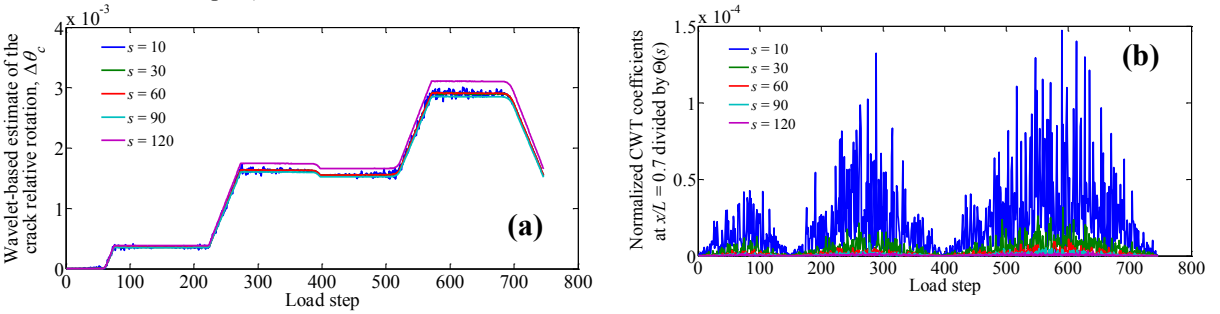

Fig. 4. (a) Histories of the crack relative rotation $\Delta\vartheta_c$ estimated by the wavelet-based calibration method; (b) normalized CWT coefficients at $x/L = 0.7$ divided by $\Theta(s)$. Different wavelet scale are used and SNR = 120 dB.

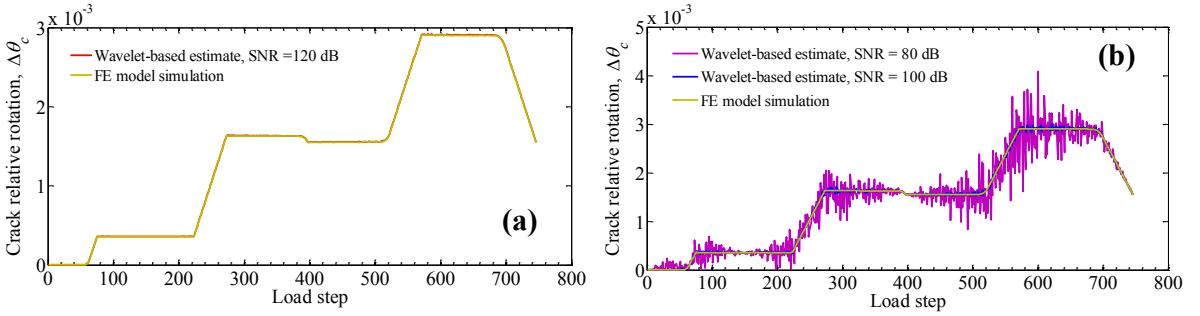

Fig. 5. Comparison of the estimate of the wavelet-based calibration method at $s = 60$ (SNR = 120 dB) and the simulation of the FE model: (a) SNR = 120 dB; (b) SNR = 80 and 100 dB.

References

Basu, B., Nagarajaiah, S., Chakraborty, A., 2008. Online identification of linear time-varying stiffness of structural systems by wavelet analysis. Structural Health Monitoring, 7(1) 21-36.

Carpinteri, A., Spagnoli, A., Vantadori, S., 2004. A fracture mechanics model for a composite beam with multiple reinforcements under cyclic bending. International Journal of Solids and Structures, 41 5499-5515.

Friedman, Z., Kosmatka, J. B., 1993. An improved two-node Timoshenko beam finite element. Computers & structures, 47(3) 473-481.

Hou, Z., Noori, M., Amand, R. S., 2000. Wavelet-based approach for structural damage detection. Journal of Engineering Mechanics, 126(7) 677-683.

Loutridis, S., Douka, E., Trochidis, A., 2004. Crack identification in double cracked beams using wavelet analysis. Journal of Sound and Vibration, 277 1025-1039.

Mallat S., 2001. A wavelet tour on signal processing. Academic Press, New York.

Montanari, L., 2014. Vibration-based damage identification in beam structures through wavelet analysis. Ph.D. Thesis, University of Parma, Parma, Italy.

Montanari, L., Basu, B., Spagnoli, A., Broderick, B. M., 2014. A padding method to reduce edge effects for enhanced damage identification using wavelet analysis. International Journal of Mechanical Systems and Signal Processing (submitted).

Pakrashi, V., Basu, B., O' Connor, A., 2007. Structural damage detection and calibration using a wavelet–kurtosis technique. Engineering Structures, 292097-2108.

Spagnoli, A., Carpinteri, A., Montanari, L., 2014. Application of the Shakedown Theory to Brittle-Matrix Fiber-Reinforced Cracked Composite Beams Under Combined Traction and Flexure. Journal of Applied Mechanics, 81(3), 031012.

Viola, E., Nobile, L., and Federici, L., 2002. Formulation of cracked beam element for structural analysis. Journal of engineering mechanics, 128(2) 220-230.